THE JOURNAL OF PHYSICAL CHEMISTRY C

Article

Cite This: J. Phys. Chem. C 2019, 123, 12195−12202

pubs.acs.org/JPCC

Photochemical Synthesis of Azoarenes from Aryl Azides on Cu(100): A Mechanism Unraveled

Published as part of The Journal of Physical Chemistry virtual special issue "Hai-Lung Dai Festschrift".

Yun-Wen Luo, Chih-Hung Chou, Po-Chiao Lin,* and Chao-Ming Chiang*

Department of Chemistry, National Sun Yat-sen University, Kaohsiung 80424, Taiwan

Supporting Information

ABSTRACT: Thermal, photochemical, and metal-facilitated routes to aryl nitrenes via the extrusion of dinitrogen from aryl azides adsorbed on a single-crystal copper surface have been investigated. Only by irradiation with UV−vis light can an N═N bond be made, rendering an azoarene. Evidence of the wavelength-dependent N−N_2 bond dissociation rates supports a photoinduced substrate-mediated electron attachment mechanism, leading concurrently to stable, spectroscopically identifiable copper/nitrene intermediates (spectators) as well as transitory reactive triplet nitrenes that readily self-couple to achieve the on-surface azo-dimer synthesis.

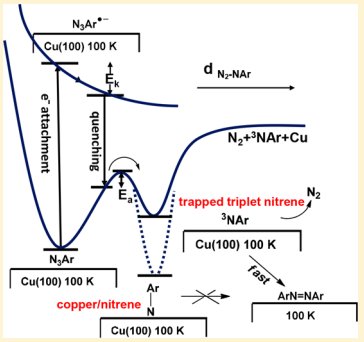

1. INTRODUCTION

On-surface synthesis, a bottom-up strategy for the fabrication of extended covalent surface-confined molecular frameworks, aims at conferring self-assembly structures the required stability for their real applications.[1−3] Its immense potential has spurred considerable research interest in investigating what classes of organic bond-forming reactions can be realized with reactants adsorbed on well-defined surfaces under ultrahigh vacuum (UHV) conditions. To date, a cornucopia of classic reactions, such as Ullmann coupling,[4,5] Sonogashira coupling,[6,7] azide−alkyne cycloaddition,[8,9] etc. has been scrutinized experimentally using a surface science approach. Nevertheless, generation of N═N bond rendering aromatic azo compounds (azoarenes ArN═NAr) directly on a metal surface, key to functionalization of surfaces with molecular switches[10−15] or incorporation of these motifs into more complex systems,[16] has yet to emerge. It is well-known that singlet nitrenes (^{1}NAr), resulting from the pyrolysis or photolysis of aryl azides (N_3Ar) with N_2 as a stoichiometric byproduct, can either undergo ring expansion to ketenimines or competing relaxation through intersystem crossing (ISC) to triplet nitrenes (^{3}NAr) which then dimerize by NN coupling to form azoarenes in solution or matrices.[17−22] In contrast, transition metal catalysis normally offers a conduit to achieve *selective* NN coupling via the intermediacy of metal-stabilized nitrene/imide. Studies have shown that transition metal complexes are particularly useful vehicles for the homogeneous catalytic azoarene synthesis from aryl azides. Intriguingly, a variety of possible pathways responsible for the ArN═NAr formation have been demonstrated, including (1) bimolecular coupling of a metal nitrene/imide (MNAr)[23−25] or a dinuclear bridging imido (μ-NAr) moiety,[26] (2) external attack of a metal nitrene/imide species by the parent aryl azide resulting in a metal-tetrazene type of intermediate or transition state that releases azoarene after N_2 extrusion (MNAr + N_3Ar → M(N_4Ar_2) → ArN═NAr + N_2),[27] and (3) rapid recombination of discrete aryl nitrenes that escaped from the metal centers.[28−30] Possible analogies between the chemistry on metal surfaces and that of organometallic complexes prompted us to look into the heterogeneous version of the azido-to-azo transformation on a single-crystal surface in a UHV environment. Herein we report an investigation of the thermal and photochemical reactions of adsorbed 4-methoxyphenyl azide (4-MPA) on a copper (100) surface. Selection of a substituted aryl azide (nonexplosive and easy to make) in conjunction with a coinage metal might yield a metal/nitrene species that would retain some stability for characterization, yet also exhibits N═N bond-forming reactivity. We used reflection−absorption infrared spectroscopy (RAIRS) to search for surface intermediates, and thermal desorption (TD) mass spectrometry to survey gas-phase products.

2. EXPERIMENTAL AND THEORETICAL METHODS

2.1. General. Experiments were performed in a UHV chamber evacuated by ion and turbomolecular pumps. The ultimate pressure below 2.0×10^{-10} Torr was reached after baking. The chamber was equipped with an ion sputtering gun for surface cleaning, a triple-filter quadrupole mass spectrometer (QMS) for detecting residual gases as well as desorbing species from the surface, RAIRS for collecting surface

Received: December 23, 2018
Revised: April 25, 2019
Published: April 26, 2019

DOI: 10.1021/acs.jpcc.8b12373
J. Phys. Chem. C 2019, 123, 12195−12202

vibrational spectra, and low energy electron diffraction (LEED) optics. The Cu(100) single-crystal sample is a 2 mm thick disk with a diameter of 12.5 mm, which was attached to a heating element on a manipulator with capabilities for resistive heating to 1100 K and active cooling to 100 K by liquid nitrogen. A K-type thermocouple with its junction wedged into a hole on the perimeter of the crystal enabled the measurement of surface temperature. Programmed heating was conducted by a PID controller to ramp the temperature in a regulated fashion. Normal TD experiments were started by exposing the Cu(100) to the vapors of the aryl azide compound at the desired surface temperature (100 or 250 K), and then the sample was positioned ∼1 cm from the apertured entrance of the QMS (enclosed in a differentially pumped housing with a pinhole to avoid collecting species from the sample holder) in a line-of-sight configuration. The surface was elevated to 800 K with a linear rate of 1.5 K/s. Upon heating, multiple-ion signals and temperatures were collected synchronously. RAIRS was performed by taking the infrared beam from a commercial FTIR spectrometer and focusing it at grazing incidence (85°) through a ZnSe wire-grid polarizer and a differentially pumped, O-ring sealed KBr window onto the copper surface in the UHV chamber. The reflected IR beam was passed through an exit KBr window and refocused on a liquid nitrogen-cooled HgCdTe detector to collect spectra between 650 and 4000 cm^{-1}. Each spectrum was obtained with 512 scans at 4 cm^{-1} resolution and ratioed against the background spectra from the clean surface. A clean and well-orderd Cu(100) surface was achieved by cycles of bombardment of Ar^+ ions and annealing at 850 K and confirmed by its sharp LEED pattern. Gas exposures were quoted as Langmuirs (1 Langmuir = 1 L = 10^{-6} Torr s), uncorrected for ionization gauge sensitivity and collimator gain factor.

2.2. Photochemical. Two light-emitting diode (LED) sources (Dr. Honle AG UV Technology, Germany) were employed, and they provided photons in the spectral region of the stated 365 ± 10 and 405 ± 10 nm ranges. The LED head was mounted on a fused silica re-entrant viewport of the chamber to bring it to a suitable focusing distance (38 mm) with a photon peak intensity estimated to be ∼750 mW/cm^2 for the 365 nm LED and ∼1500 mW/cm^2 for the 405 nm LED. The light directly shined through the window to give an irradiation spot of ∼20 mm in diameter which covers the whole surface area. No obvious temperature rise was registered when the sample was irradiated at 100 K. Postirradiation TD measurements or mass response as a function of irradiation time was conducted by positioning the sample face normal to the QMS aperture and 45° to the light source.

2.3. Sample Preparation. 4-Methoxyphenyl azide (4-MPA) and 2,6-difluorophenyl azide (2,6-DFPA) were synthesized according to the literature procedures[31] and purified by silica gel column chromatography with an ethyl acetate/hexane system. These azides were stored at −40 °C until immediately prior to use. During experiments the solid azide samples were processed in a gas-handling manifold pumped by diffusion and rotary vane pumps, and were sublimed directly from a sample tube at room temperature under 10^{-5} Torr vacuum. A tubular doser connected to a precision leak valve can accurately control the vapor exposures of azides. Mass spectra were routinely measured while dosing. After comparing them with the mass spectra documented in the Chemistry Webbook from NIST, the purity of the reagents was verified (see the data in Figure S1 for 4-MPA in Supporting Information).

2.4. Computational. The calculations, including structure optimization and vibrational frequency analysis, were performed with the density functional theory (DFT) method at the restricted and unrestricted B3LYP level of theory as implemented in Gaussian 09 program package.[32] We employed the 6-31G(d) + LANL2DZ mixed basis set that utilizes the Los Alamos Effective Core Potential on the transition metal, while utilizing a Pople-type basis set on all other atoms. A more sophisticated Stuttgart−Dresden ECP D-basis set (SDD) was tested, and there was not a big advantage to using SDD in terms of accuracy; therefore, we decide to stick with LANL2DZ for the sake of computation speed. The Cu(100) surface was mainly modeled by a 5 × 5 single-layer Cu_{25} cluster (25 represents the number of the surface atoms). The number of surface layer and overall cluster size were a compromise between accuracy and cost in modeling all the adsorbate/surface complexes involved. The surface-bound aryl azides, aryl nitrenes, and azoarenes were attached to the Cu cluster with its Cu−Cu distance fixed at 2.556 Å, while the C, N, O, F, and H atoms were unconstrained and allowed to optimize. All geometries were optimized fully without symmetry constraints. Frequency calculations were performed to confirm the nature of the stationary points and to obtain zero-point energies. The frequencies given were scaled by a factor of 0.961 to compensate for the absence of anharmonicity in this type of computation.[33] The GaussView visualization program was used to picture the normal modes for vibration assignments. We calculated the total energy of the free neutral N_3Ar moelcule at its optimized geometry and the energy of the radical anion by adding one electron to the neutral (changing the net charge to −1) and the spin multiplicity ($2S + 1 = 2$ for a doublet) with the same method/basis set at the optimized geometry of the neutral, and then subtracting the two energies to obtain the gas-phase vertical electron affinity (VEA).

3. RESULTS AND DISCUSSION

3.1. Thermal Chemistry. When 4-MPA was deposited onto a Cu(100) surface held at 250 K, a species having intense IR bands at 1595, 1489, 1290, and 1250 cm^{-1} can be readily assigned to a high coordination aryl nitrene in the 4-fold hollow site (see Figure 1a) based on the excellent spectral agreement with the results from DFT calculations using the single-layer Cu_{25} model (Figure 2a,b). The observed and computed frequencies in conjunction with mode assignments are summarized in Table 1. A two-layer cluster model

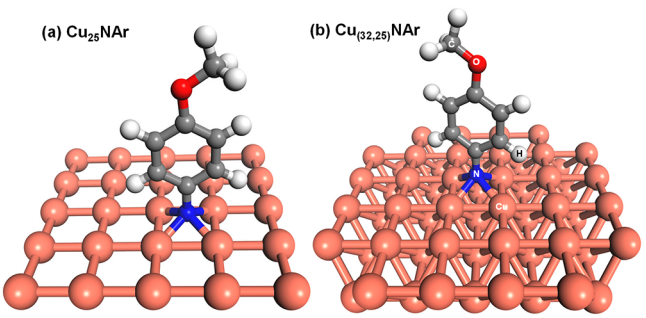

Figure 1. DFT optimized geometric structures of a single 4-methoxyphenyl nitrene unit on top of Cu(100)-like single-layer Cu_{25} (a) and two-layer $Cu_{(32,25)}$ clusters (b).

DOI: 10.1021/acs.jpcc.8b12373
J. Phys. Chem. C 2019, 123, 12195−12202

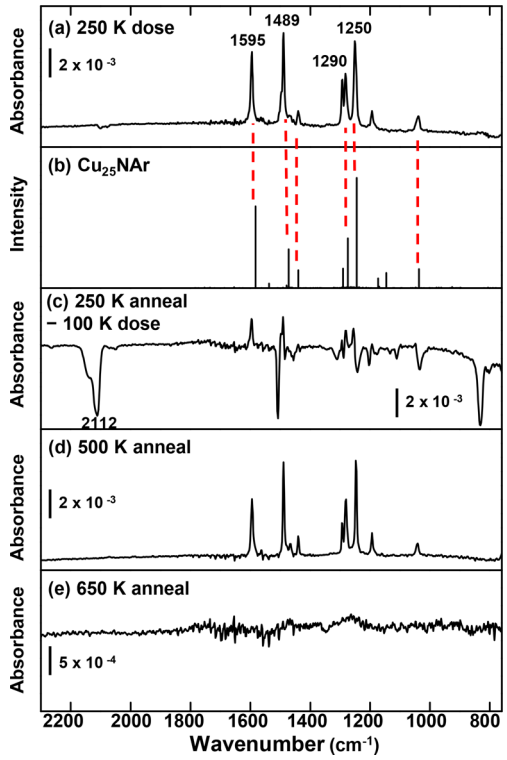

Figure 2. (a) RAIR spectrum of surface species isolated by exposing Cu(100) to 1 L 4-MPA at 250 K. (b) DFT calculated spectrum from the modeled complex in Figure 1a. (c) Difference spectrum showing the thermolysis of 4-MPA (negative peaks) upon 250 K annealing and the resultant CuNAr intermediate (positive peaks). (d, e) Spectra obtained by further annealing to the indicated temperatures.

Table 1. Observed and Calculated IR Frequencies (cm^{-1}) for CuNAr, Ar = 4-$MeOC_6H_4$

mode[a]	on Cu(100)	on Cu_{25} cluster by DFT[b]
ring CC str; CH_3 sym def	1595	1582
CH ip bend; CH_3 asym def	1489	1472
CH ip bend; CH_3 asym def	1440	1439
ring CO str; CH ip bend	1290	1274
ring CO str; CH ip bend	1250	1244
ring CN str; CH ip bend	1200	1172, 1145
O–CH_3 str	1034	1036

[a]Definite individual assignments are difficult because of mode coupling: str = stretch; sym = symmetric; def = deformation; asym = asymmetric; ip = in plane. [b]Scaled by 0.961.

containing 57 Cu atoms (32 and 25 on the first and second layer, respectively) denoted as $Cu_{(32,25)}$ adopted in a study by Piantek et al.[34] for a similar copper-surface-bound aryl nitrene unit was also put to a test. We managed to optimize a geometry, displayed in Figure 1b, using crude convergence criteria conver = 5 in the Gaussian 09 package. The proclivity for the 4-methoxyphenyl nitrene moiety bound to the metal framework in a multinuclear fashion is confirmed by both the single- and two-layer cluster models, thus duplicating the preferred adsorption site in the previous work.[34] Tighter convergence criteria were attempted, but convergence of the wave functions for such a large system was slow (costly as well). A more refined structure and the resulting frequency calculations are unsuccessful at the present time. The same surface-bonded species can be reproduced experimentally by exposing Cu(100) to 1 L 4-MPA at 100 K followed by annealing to 250 K. Here, 1 L was our highest exposure to render a single molecular desorption peak (see Figure S2 for the coverage-dependent TD spectra), and saturation of the monolayer evidently occurred between 1 and 2 L. As illustrated in the difference spectrum (Figure 2c), the downward bands, especially the strong asymmetric N_3 stretching mode at 2112/2130 cm^{-1} (split due to a Fermi resonance), are indicative of the depletion of parent 4-MPA by heat. Four major upward peaks are concomitantly observed; their positions and shapes are identical to those in Figure 2a. Figure 2d demonstrates that the resultant multinuclear copper/nitrene complex (CuNAr, Ar = 4-$MeOC_6H_4$) as suggested by the theory remains thermally stable up to 500 K; however, further heating must trigger successive reactions to dispose of the vibration features of the entire spectrum (see Figure 2e taken after the 650 K anneal). TD measurements (Figure 3) showed desorption of

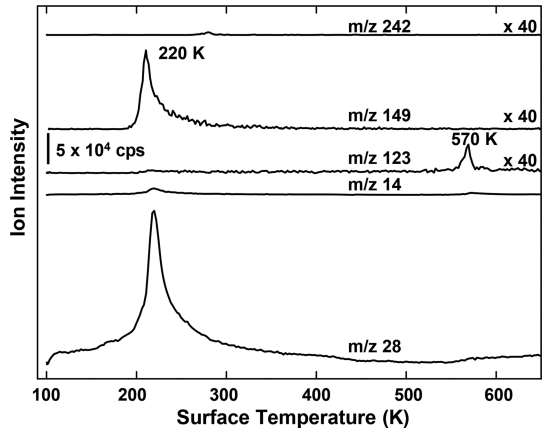

Figure 3. Multiplex TD spectra after adsorption of 1 L 4-MPA on Cu(100) at 100 K.

intact molecules characterized by m/z 149 (parent ion of 4-MPA, N_3Ar) near 220 K, but some azides underwent ArN–N_2 bond scission to extrude N_2, as evidenced by its m/z 28 and 14 fragment ion signals. The lack of desorption feature at m/z 242 (parent ion of ArN═NAr) is noteworthy, suggesting that azoarene was not the fate of CuNAr. Instead, as revealed by the m/z 123 TD profile at 570 K, aniline ($ArNH_2$) was produced, presumably via H atom abstraction from the phenyl ring of a neighboring metal/nitrene counterpart (see Scheme 1a).[35] Dissociative adsorption of the background H_2 is highly activated on copper surfaces and will not serve as the source of H atoms. The failure to discover the formation of azo compound indicates that metal/nitrenes are not labile enough to undergo NN coupling.

3.2. Photochemistry. Control experiments demonstrated that photons were required for making azoarenes. The photochemical processes were conveniently enabled by using UV–vis light-emitting diodes (LEDs). Irradiation of the 100 K physisorbed 4-MPA at 405 or 365 nm for 10 min resulted in RAIR spectra (Figure 4b,c) that are fairly different from the one without UV exposure (Figure 4a). Photolysis was readily inferred by the diminished (405 nm) or vanished (365 nm) N_3 azido vibration features near 2100 cm^{-1}. To diagnose the possible light-induced ejection of species, line-of-sight mass spectrometer response as a function of irradiation time was monitored. Figure 5a,b exhibits the rise-and-fall pattern of m/z 28 corresponding to the N_2 appearance and disappearance

DOI: 10.1021/acs.jpcc.8b12373
J. Phys. Chem. C 2019, 123, 12195–12202

Scheme 1. On-Surface Reaction Scenarios: (a, b) Outcome of Thermal and Photochemical Reactions and (c, d) Two Viable Pathways To Forge N═N Bond, but the Former Was Discounted Experimentally (see Figure 8)

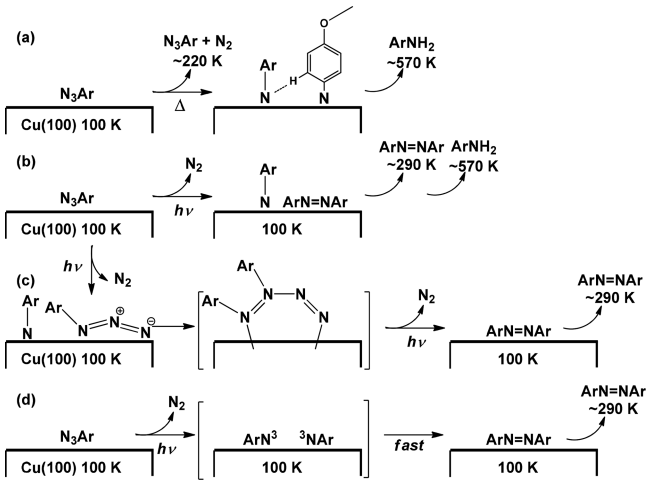

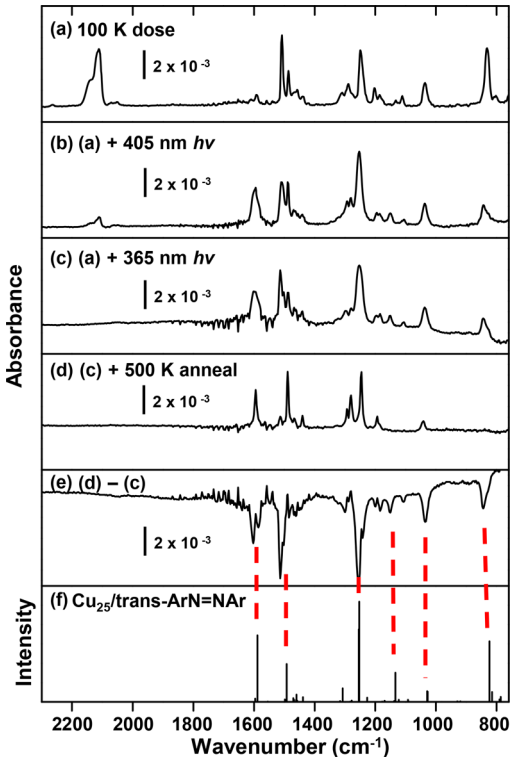

Figure 4. (a) RAIR spectrum of 1 L physisorbed 4-MPA at 100 K. (b, c) Spectra measured after photoirradiation with UV–vis LEDs. (d) Postirradiation spectrum (c) subjected to 500 K anneal. (e) Difference spectrum showing the escaped photolysis product (negative peaks) by annealing. (f) Calculated spectrum from DFT optimized Cu_{25}/*trans*-azoarene structure (see Figure 6).

upon turning the LED on and off. The relatively flat decay profile at 405 nm implies a slower reaction rate and explains why the photodissociation of 4-MPA at 405 nm was not quite complete, as displayed by the residual N_3 signals in RAIRS (Figure 4b). Following N_2 split-off by photolysis at 365 nm, there are in fact two surface species present in the postirradiation spectrum (Figure 4c) bearing rather broad IR features. One of them survived the 500 K anneal giving rise to

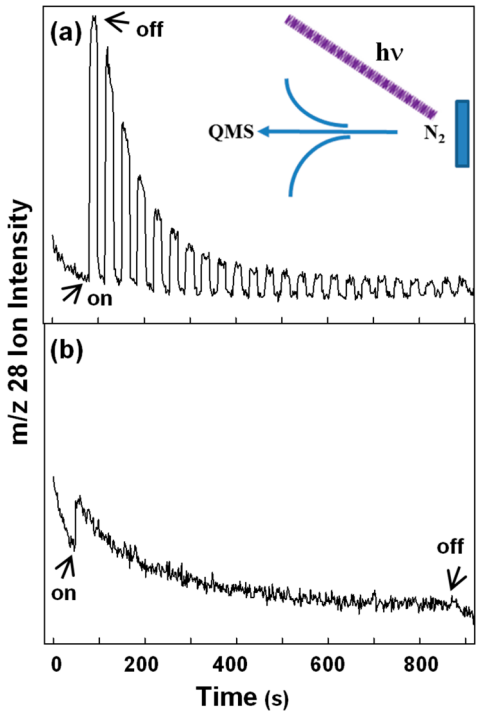

Figure 5. QMS responses of N_2 ejection as a function of irradiation time obtained during the photolysis at (a) 365 nm (photon flux ~1.38 × 10^{19} photons/s cm^2) and (b) 405 nm (photon flux ~3.05 × 10^{19} photons/s cm^2). The sharp rise is due to switching the irradiation on. The repetitive rise-and-fall pattern in part a corresponding to intentionally turning the LED on and off every 15 s confirms that the decay profile is a result of light exposure rather than background pressure change. The intensity scales in parts a and b are the same.

a spectrum (Figure 4d) which resembles Figure 2d quite closely; therefore, it can be unequivocally attributed to the aforementioned CuNAr. The identity of the other species can be uncovered by taking a difference spectrum between Figure 4d,c. Bands pointing downward in the resulting spectrum (Figure 4e) stand for the photoproduct that escaped from Cu(100) during annealing, and all of them correlate reasonably well with the spectrum (Figure 4f) calculated for flat-lying *trans*-azoarene bound to a Cu_{25} cluster (Figure 6). The observed and computed frequencies along with mode assignments are listed in Table 2. Even so, we cannot entirely exclude the possibility that some *cis*-azoarenes also exist (see data in Table S1 of Supporting Information for comparison). We made an effort to synthesize the authentic ArN═NAr which was not easily sublimed; thus, acquisition of the RAIR spectrum directly from adsorbed azo molecules was unsuccessful. Postirradiation TD (PITD) measurements, Figure 7, indeed observed the evolution of ArN═NAr (m/z 242) near 300 K along with the self-hydrogenated product (m/z 123 for $ArNH_2$) at ~570 K (Scheme 1b). The absence of m/z 149 (N_3Ar) and 28 and 14 (N_2) corroborates that adsorbed 4-MPA thoroughly dissociates under irradiation.

Although resistant to NN coupling, copper/nitrene might still interact with unreacted aryl azide to form a metal tetrazine complex which rapidly denitrogenates to yield the azo-dimer photochemically. We view this as an example of the 1,3-dipolar cycloaddition of an organic azide to an unsaturated metal–nitrogen bond (Scheme 1c). Several precedents for such reactions were found in the literature.[27,36,37] To test this route, we contrived a crossover experiment involving a separate aryl

DOI: 10.1021/acs.jpcc.8b12373
J. Phys. Chem. C 2019, 123, 12195–12202

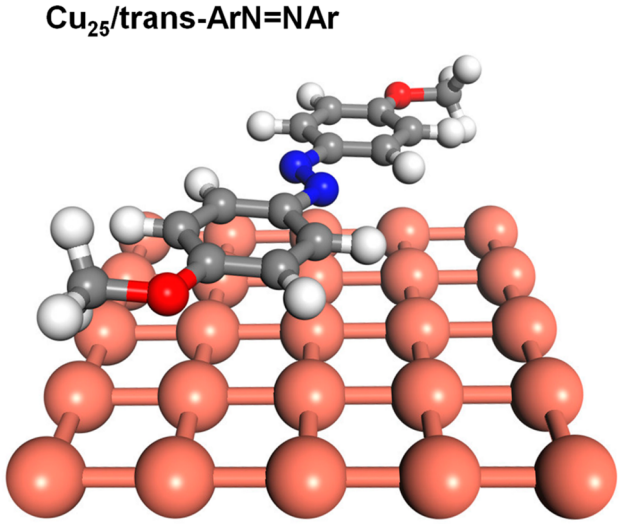

Figure 6. DFT optimized geometric structure of Cu_{25}/*trans*-azoarene.

Table 2. Observed and Calculated IR Frequencies (cm^{-1}) for *trans*-ArN═NAr, Ar = 4-$MeOC_6H_4$

mode[a]	on Cu(100)	on Cu_{25} cluster by DFT[b]
ring CC str	1603	1588
CH ip bend; CH_3 sym def	1514	1492
ring CO str; ring breath	1255	1253
CH ip bend	1151	1134
O−CH_3 str	1036	1029
CH op bend	845	824

[a]Definite individual assignments are difficult because of mode coupling: str = stretch; sym = symmetric; def = deformation; ip = in plane; op= out of plane. [b]Scaled by 0.961.

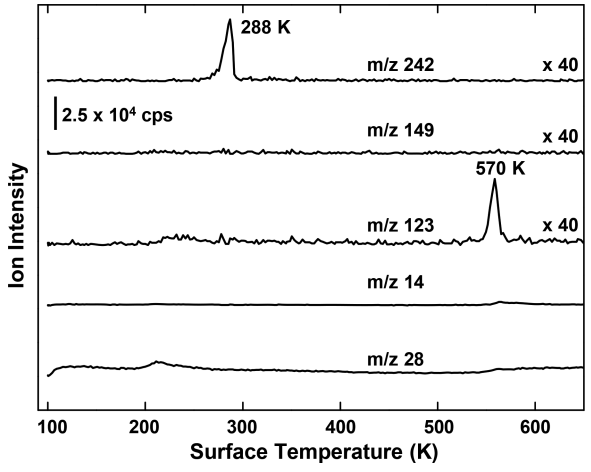

Figure 7. The 365 nm postirradiation multiplex TD spectra following 1 L 4-MPA adsorption at 100 K.

azide; hence, 2,6-difluorophenyl azide (2,6-DFPA, N_3Ar', Ar′ = 2,6-$C_6H_3F_2$) was synthesized for this purpose. First, a control experiment, in which a 0.5 L/0.5 L mixture of 4-MPA and 2,6-DFPA was deposited on Cu(100) at 100 K followed by 10 min of 365 nm UV illumination, was performed. PITD detected a mixture of ArN═NAr/Ar′N═NAr/Ar′N═NAr′ according to their parent *m*/*z* 242, 248, and 254 ion signals, respectively (Figure 8a). Next, CuNAr was isolated in advance by dosing 0.5 L N_3Ar onto the copper surface held at 250 K, which was

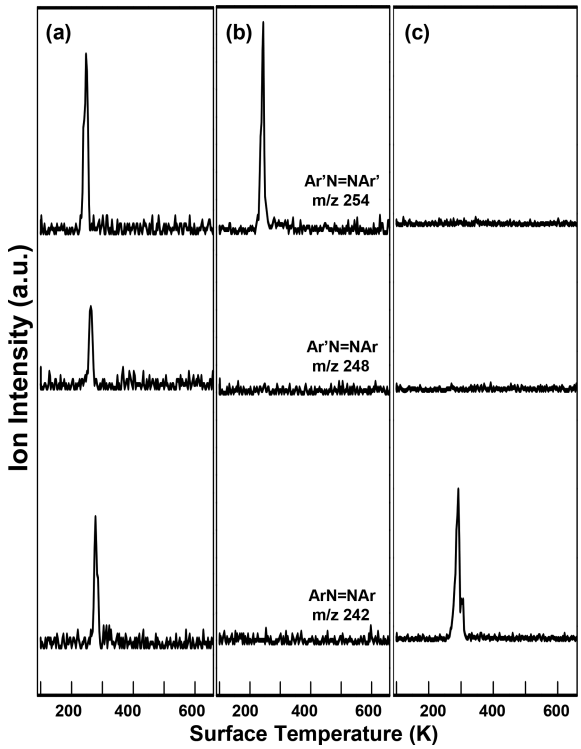

Figure 8. (a) Postirradiation TD spectra of three possible azoarenes taken after coadsorption of 0.5 L 4-MPA and 0.5 L 2,6-DFPA on Cu(100) at 100 K. (b) Postirradiation TD spectra of self-coupled and cross-coupled azoarenes taken after sequential adsorption of 0.5 L 4-MPA at 250 K and 0.5 L 2,6-DFPA at 100 K on Cu(100). (c) Same as part b, except that the order of the adspecies was reversed.

succeeded by coadsorption of N_3Ar' as well as 10 min of UV exposure at 100 K. If 1,3-dipolar addition was truly attributable to azoarene formation, the hetero Ar′N═NAr would be observable to some extent in the PITD spectra. It turned out that only one homocoupled azoarene Ar′N═NAr′ was discovered in Figure 8b (symmetric ArN═NAr should not be expected). As the order of coadsorption was reversed, the results were essentially the same; namely, Ar′N═NAr was also not accessible (Figure 8c). We thus discounted the pathway in Scheme 1c that entails a reactive metallacyle intermediate/transition state.

The third alternative to the mechanistic scenario would be the facile recombination of nascent aryl nitrenes by photolysis (Scheme 1d). It is well-established that triplet aryl nitrenes react with themselves to yield azoarenes. The consensus is that this reactivity (behaving like 1,1-diradicals) is unique to the triplet state.[38] If singlet nitrene is released, it would undergo ISC to triplet nitrene.[39,40] In this case, ISC would have to be accelerated by the influence of nearby surface metal centers because metal coordination imparting internal heavy atoms carrying large orbital angular momentum facilitates ground triplet state production.[41] This formal nitrene−nitrene coupling route not only explains the outcome that a mixture of three distinct azoarenes was created upon UV irradiation of the composite containing two different physisorbed aryl azides at 100 K (Figure 8a), but also circumvents the involvement of chemisorbed CuNAr.

3.3. Photodissociation Processes. Photodissociation must involve electronic transitions that sever bonding between the nitrogen proximal to the aromatic ring and a distal N_2

DOI: 10.1021/acs.jpcc.8b12373
J. Phys. Chem. C 2019, 123, 12195−12202

moiety. Recently McMahon et al. reported that irradiation of 4-MPA in an argon matrix at 10 K with light of λ = 365 nm can lead to formation of triplet nitrene which was unstable upon further irradiation (λ = 313 or >415 nm).[22] However, the reactivity dependence on the photon energy was not discussed. We considered two possible courses: in one path, the photon is deposited directly within the weakly bound adsorbate and triggers an electronic transition to its excited π^* state where the electron density is found to be localized in the N_3 unit (see the calculated LUMO orbital in Figure S4). It was deemed advisible to examine the optical absorption spectrum of 4-MPA (Figure S5) which exhibits two components: a strong band (λ_{max} = 252 nm) and a weak long wavelength shoulder band at 290 nm. Therefore, the photon energies utilized (365 or 405 nm) are clearly not sufficient to induce an intra-adsorbate excitation unless the energy levels of azide were significantly shifted due to adsorption. As the IR spectrum of monolayer 4-MPA on Cu(100) taken at the photolysis temperature was found to coincide well with that of the bulk sample, we do not expect interaction with the solid to be substantial. The energy levels of the adsorbate should be relatively unperturbed so that direct photon absorption is not the operative mechanism.

The second model is based on a substrate-mediated electron transfer process whereby photoexcited hot electrons in the Cu subvacuum continuum lead to a transient negative ion (attachment of an electron to the adsorbate LUMO affinity level) that is unstable toward dissociation.[42] To determine the amount of excitation above the Fermi level one needs for resonant attachment, the position of LUMO is an important factor. First, it is assumed that the vacuum levels (E_v) of two materials in contact (adsorbate/substrate) align, as shown in Figure 9a. We begin by using the computationally determined vertical electron affinity (VEA(g) = −1.29 eV, see data in Table S1) to position the LUMO level of the gas-phase N_3Ar with respect to the E_v of the system.[43] The negative sign implies that the molecule is less stable with the electron attached; therefore, the LUMO of the isolated molecule lies above the vacuum level. Harrison et al.[44] have argued that the unoccupied affinity level for physically adsorbed molecules would be subjected to image charge attraction in front of a conductor and electronic polarization of the surrounding adspecies. Both effects translate into a downshift of the energy level. The image charge stabilization energy is $E_{im} = e^2/4z = (3.6/z)$ eV, where z is the distance between the adsorbate and the metal surface expressed in angstroms. For z = 3.7 Å (from the calculated structure of 4-MPA/Cu_{25} in Table S1), one finds E_{im} is about 0.97 eV. The polarization energy $E_{pol} = (e^2/2r)(1 - 1/\varepsilon)$ depends on the dielectric constant (ε) and varies inversely with the size of the adsorbate (r). Given ε = 8.84 (using the value of 4-methoxy aniline instead) and r = 5.12 Å, E_{pol} is crudely estimated to be 1.25 eV for a monolayer of 4-MPA. The combined influences of E_{im} and E_{pol} thus bring the LUMO back to about 0.93 eV below the vacuum level. The work function of a clean Cu(100) is 4.59 eV,[45] but the work function change by a monolayer 4-MPA on Cu(100) is not known. An estimate of −1.0 eV was taken from the case of benzene on Cu(111) because the rings of 4-MPA and benzene all adopt the similar flat-lying mode of adsorption.[46] Then, the work function of Cu(100) covered by a monolayer of 4-MPA is assumed to be 3.59 eV. As depicted in Figure 9a, we expect to find the affinity level that is situated at about 2.66 eV above the Fermi level (E_F). This is within the reach of the 365 nm (3.38 eV) and 405 nm (3.05 eV) photons which promote the

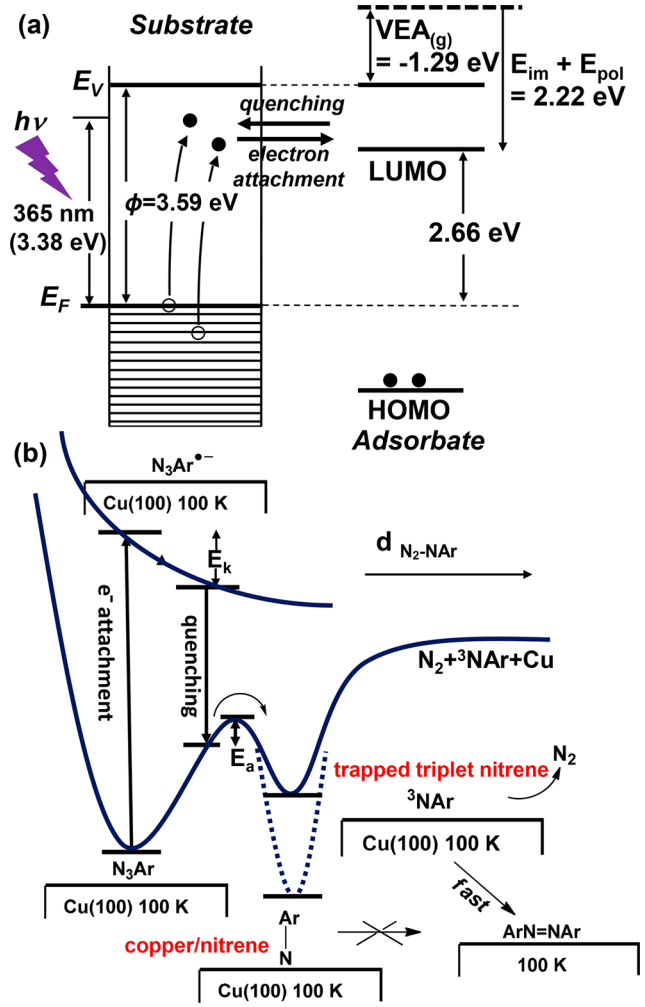

Figure 9. (a) Schematic diagram illustrating photon-induced electron attachment process between metal substrate and adsorbate. The electron affinity level (LUMO) position is estimated for its accessibility. (b) Schematic PE curves for intra-adsorbate bond dissociation coupled to those for trapping and chemisorption of the photoproducts.

electrons from the Fermi level and below to energies in the range required for resonant attachment. In fact, Germer et al. calculated the hot electron energy distribution of the joint density of states $D(E, h\nu)$ created by 578 nm (2.14 eV) and 289 nm (4.29 eV) on Cu(100) from the copper band structure.[47] According to their results, 4.29 eV photons can generate a significant number of hot electrons up to 2.7 eV above E_F from a filled d to empty sp band transition. Therefore, photon energies in the vicinity of 3 eV are needed to create a substantial amount of nascent electrons at energies near the LUMO. Especially 365 nm (3.38 eV), photons should produce a hot electron distribution that is better matched to the unoccupied adsorbate state than 405 nm (3.05 eV) photons. This wavelength-dependent argument is clearly reflected in an elevated photolysis rate at 365 nm compared to that at 405 nm (see the decay curves in Figure 5), despite the fact that the 365 nm LED provided a somewhat lower photon flux (see Figure 5 caption). The photochemical events continue to unfold along the potential energy (PE) curves for the N_2−N bond dissociation process as shown in Figure 9b. Upon attachment, transitory aryl azide radical anions ($N_3Ar^{\bullet-}$)

DOI: 10.1021/acs.jpcc.8b12373
J. Phys. Chem. C 2019, 123, 12195−12202

are created. The captured electron occupies the antibonding orbital (LUMO), and the $[N_2{-}NAr]^{\bullet-}$ interaction is often repulsive. Consequently, the N_2 and $NAr^{\bullet-}$ (aryl nitrene radical anion) start to move apart on the upper PE curve and eventually dissociate to liberate nitrogen and form the adsorbed aryl nitrene radical anion. Yet, it is quite unlikely that $NAr^{\bullet-}$(ad) undergoes NN coupling to give azoarene, due to the severe energetic penalty for paring up anionic species. A more plausible scenario is that, after a nuclear motion of $[N_2{-}NAr]^{\bullet-}$ on a time scale of the radical anion lifetime, quenching brings it back to the ground neutral $N_2{-}NAr$ PE surface. If the amount of kinetic energy E_k gained on the excited PE surface is higher than E_a, crossover of the vibrationally excited $N_2{-}NAr$ to a trapped triplet nitrene ^3NAr(ad) and chemisorbed CuNAr may occur even at the 100 K photolysis temperature. The active nitrenes can readily recombine to afford ArN═NAr(ad).

4. CONCLUSIONS

In summary, the work herein adds to the repertoire of on-surface synthesis of covalent bonds and showcases the first realization of photochemical activation of adsorbed aryl azides to achieve the selective N═N bond formation producing azoarenes on a two-dimensional confined metal surface under UHV conditions. Although both thermolysis and photolysis of a surface-bound aryl azide can lead to the isolation of a stable and spectroscopically identifiable copper/nitrene moiety, NN coupling mechanisms involving the interactions between this intermediate and itself or a parent aryl azide via 1,3-dipolar cycloaddition have been ruled out. Instead, highly reactive triplet aryl nitrenes are invoked, and rapid dimerization at the site of their generation delivers azoarenes. Photodissociation is indirectly induced by hot electron (generated in the substrate by photons) attachment to form temporary anions prone to the $N_2{-}N$ bond dissociation. After a short lifetime the electrons decay back to metal while the adsorbates return to a vibrationally hot ground-state and easily surmount the barrier into the dissociatively trapped/chemisorbed states. Photo-irradiation is mandatory to make N═N covalent bonds; therefore, harnessing the power of near-field optical probes to enable direct writing or nanopatterning of azobenzene-type molecular switches on surfaces is envisaged.

■ ASSOCIATED CONTENT

Supporting Information

The Supporting Information is available free of charge on the ACS Publications website at DOI: 10.1021/acs.jpcc.8b12373.

> Mass pattern of 4-MPA; coverage-dependent molecular desorption of 4-MPA; multiple-ion TD spectra after 2,6-DFPA adsorption on Cu(100); calculated HOMO and LUMO orbitals; UV−vis spectrum of 4-MPA; optimized structures, total energies, and vibrational spectra of various species involved (PDF)

■ AUTHOR INFORMATION

Corresponding Authors

*E-mail: pclin@mail.nsysu.edu.tw.
*E-mail: cmc@mail.nsysu.edu.tw.

ORCID

Po-Chiao Lin: 0000-0001-9895-2306
Chao-Ming Chiang: 0000-0002-5021-9612

Notes

The authors declare no competing financial interest.

■ ACKNOWLEDGMENTS

We acknowledge the funding from Ministry of Science and Technology, Taiwan, Republic of China, under Grants MOST105-2113-M-110-005 and MOST106-2113-M-110-008.

■ REFERENCES

(1) Shen, Q.; Gao, H.-Y.; Fuchs, H. Frontiers of On-Surface Synthesis: From Principles to Applications. *Nano Today* **2017**, *13*, 77−96.

(2) Held, P. A.; Fuchs, H.; Studer, A. Covalent-Bond Formation via On-Surface Chemistry. *Chem. - Eur. J.* **2017**, *23*, 5874−5892.

(3) Fan, Q.; Gottfried, J. M.; Zhu, J. Surface-Catalyzed C-C Covalent Coupling Strategies toward the Synthesis of Low-Dimensional Carbon-Based Nanostructures. *Acc. Chem. Res.* **2015**, *48*, 2484−2494.

(4) Hla, S.-W.; Bartels, L.; Meyer, G.; Rieder, K.-H. Inducing All Steps of a Chemical Reaction with the Scanning Tunneling Microscope Tip: Towards Single Molecule Engineering. *Phys. Rev. Lett.* **2000**, *85*, 2777−2780.

(5) Di Giovannantonio, M.; Tomellini, M.; Lipton-Duffin, J.; Galeotti, G.; Ebrahimi, M.; Cossaro, A.; Verdini, A.; Kharche, N.; Meunier, V.; Vasseur, G.; Fagot-Revurat, Y.; Perepichka, D. F.; Rosei, F.; Contini, G. Mechanistic Picture and Kinetic Analysis of Surface-Confined Ullmann Polymerization. *J. Am. Chem. Soc.* **2016**, *138*, 16696−16702.

(6) Kanuru, V. K.; Kyriakou, G.; Beaumont, S. K.; Papageorgiou, A. C.; Watson, D. J.; Lambert, R. M. Sonogashira Coupling on an Extended Gold Surface in Vacuo: Reaction of Phenylacetylene with Iodobenzene on Au(111). *J. Am. Chem. Soc.* **2010**, *132*, 8081−8086.

(7) Sanchez-Sanchez, C.; Orozco, N.; Holgado, J. P.; Beaumont, S. K.; Kyriakou, G.; Watson, D. J.; Gonzalez-Elipe, A. R.; Feria, L.; Fernández Sanz, J.; Lambert, R. M. Sonogashira Cross-Coupling and Homocoupling on a Silver Surface: Chlorobenzene and Phenylacetylene on Ag(100). *J. Am. Chem. Soc.* **2015**, *137*, 940−947.

(8) Bebensee, F.; Bombis, C.; Vadapoo, S.-R.; Cramer, J. R.; Besenbacher, F.; Gothelf, K. V.; Linderoth, T. R. On-Surface Azide-Alkyne Cycloaddition on Cu(111): Does it "Click" in Ultrahigh Vacuum? *J. Am. Chem. Soc.* **2013**, *135*, 2136−2139.

(9) Diaz Arado, O.; Mönig, H.; Wagner, H.; Franke, J.-H.; Langewisch, G.; Held, P. A.; Studer, A.; Fuchs, H. On-Surface Azide-Alkyne Cycloaddition on Au(111). *ACS Nano* **2013**, *7*, 8509−8515.

(10) Yu, X.; Wang, Z.; Buchholz, M.; Füllgrabe, N.; Grosjean, S.; Bebensee, F.; Bräse, S.; Wöll, C.; Heinke, L. Cis-to-Trans Isomerization of Azobenzene Investigated by Using Thin Film of Metal-Organic Frameworks. *Phys. Chem. Chem. Phys.* **2015**, *17*, 22721−22725.

(11) Bronner, C.; Priewisch, B.; Rück-Braun, K.; Tegeder, P. Photoisomerization of an Azobenzene on the Bi(111) Surface. *J. Phys. Chem. C* **2013**, *117*, 27031−27038.

(12) Bazarnik, M.; Henzl, J.; Czajka, R.; Morgenstern, K. Light Driven Reactions of Single Physisorbed Azobenzenes. *Chem. Commun.* **2011**, *47*, 7764−7766.

(13) Leyssner, F.; Hagen, S.; Ovári, L.; Dokic, J.; Saalfrank, P.; Peters, M. V.; Hecht, S.; Klamroth, T.; Tegeder, P. Photoisomerization Ability of Molecular Switches Adsorbed on Au(111): Comparison between Azobenzene and Stilbene Derivatives. *J. Phys. Chem. C* **2010**, *114*, 1231−1239.

(14) McNellis, E.; Meyer, J.; Baghi, A. D.; Reuter, K. Stabilizing a Molecular Switch at Solid Surfaces: A Density Functional Theory Study of Azobenzene on Cu(111), Ag(111), and Au(111). *Phys. Rev. B: Condens. Matter Mater. Phys.* **2009**, *80*, 035414.

(15) Henningsen, N.; Rurali, R.; Franke, K. J.; Fernández-Torrente, I.; Pascual, J. I. Trans to Cis Isomerization of an Azobenzene

DOI: 10.1021/acs.jpcc.8b12373
J. Phys. Chem. C 2019, 123, 12195−12202

Derivative on a Cu(100) Surface. *Appl. Phys. A: Mater. Sci. Process.* **2008**, *93*, 241−246.
(16) Yagai, S.; Karatsu, T.; Kitamura, A. Photocontrollable Self-Assembly. *Chem. - Eur. J.* **2005**, *11*, 4054−4063.
(17) Borden, W. T.; Gritsan, N. P.; Hadad, C. M.; Karney, W. L.; Kemnitz, C. R.; Platz, M. S. The Interplay of Theory and Experiment in the Study of Phenylnitrene. *Acc. Chem. Res.* **2000**, *33*, 765−771.
(18) Gritsan, N. P.; Platz, M. S. Kinetics, Spectroscopy, and Computational Chemistry of Arylnitrenes. *Chem. Rev.* **2006**, *106*, 3844−3867.
(19) Ribblett, A. Q.; Poole, J. S. A Laser Flash Photolysis Study of Azo-Compound Formation from Aryl Nitrenes at Room Temperature. *J. Phys. Chem. A* **2016**, *120*, 4267−4276.
(20) Grote, D.; Sander, W. Photochemistry of Fluorinated 4-Iodophenylnitrenes: Matrix Isolation and Spectroscopic Characterization of Phenylnitrene-4-yls. *J. Org. Chem.* **2009**, *74*, 7370−7382.
(21) Pritchina, E. A.; Gritsan, N. P.; Bally, T. Matrix Isolation and Computational Study of the Photochemistry of *p*-Azidoaniline. *Phys. Chem. Chem. Phys.* **2006**, *8*, 719−727.
(22) Inui, H.; Sawada, K.; Oishi, S.; Ushida, K.; McMahon, R. J. Aryl Nitrene Rearrangements: Spectroscopic Observation of a Benzazirine and Its Ring Expansion to a Ketenimine by Heavy-Atom Tunneling. *J. Am. Chem. Soc.* **2013**, *135*, 10246−10249.
(23) Mankad, N. P.; Müller, P.; Peters, J. C. Catalytic N-N Coupling of Aryl Azides to Yield Azoarenes via Trigonal Bipyramid Iron-Nitrene Intermediates. *J. Am. Chem. Soc.* **2010**, *132*, 4083−4085.
(24) Zarkesh, R. A.; Ziller, J. W.; Heyduk, A. F. Four-Electron Oxidative Formation of Aryl Diazenes Using a Tantalum Redox-Active Ligand Complex. *Angew. Chem., Int. Ed.* **2008**, *47*, 4715−4718.
(25) Yiu, S.-M.; Lam, W. W.; Ho, C.-M.; Lau, T.-C. Facile NN Coupling of Manganese(V) Imido Species. *J. Am. Chem. Soc.* **2007**, *129*, 803−809.
(26) Powers, I. G.; Andjaba, J. M.; Luo, X.; Mei, J.; Uyeda, C. Catalytic Azoarene Synthesis from Aryl Azides Enabled by a Dinuclear Ni Complex. *J. Am. Chem. Soc.* **2018**, *140*, 4110−4118.
(27) Harrold, N. D.; Waterman, R.; Hillhouse, G. L.; Cundari, T. R. Group-Transfer Reactions of Nickel-Carbene and − Nitrene Complexes with Organoazides and Nitrous Oxide that Form New C = N, C = O, and N = N Bonds. *J. Am. Chem. Soc.* **2009**, *131*, 12872−12873.
(28) Bellow, J. A.; Yousif, M.; Cabelof, A. C.; Lord, R. L.; Groysman, S. Reactivity Modes of an Iron Bis(alkoxide) Complex with Aryl Azides: Catalytic Nitrene Coupling vs Formation of Iron(III) Imido Dimers. *Organometallics* **2015**, *34*, 2917−2923.
(29) Takaoka, A.; Moret, M.-E.; Peters, J. C. A Ru(I) Metalloradical That Catalyzes Nitrene Coupling to Azoarenes from Arylazides. *J. Am. Chem. Soc.* **2012**, *134*, 6695−6706.
(30) Abu-Omar, M. M.; Shields, C. E.; Edwards, N. Y.; Eikey, R. A. On the Mechanism of the Reaction of Organic Azides with Transition Metals: Evidence for Triplet Nitrene Capture. *Angew. Chem., Int. Ed.* **2005**, *44*, 6203−6207.
(31) Hu, M.; Li, J.; Yao, S. Q. In Situ "Click" Assembly of Small Molecule Matrix Metalloprotease Inhibitors Containing Zinc-Chelating Groups. *Org. Lett.* **2008**, *10*, 5529.
(32) Frisch, M. J.; Trucks, G. W.; Schlegel, H. B.; Scuseria, G. E.; Robb, M. A.; Cheeseman, J. R.; Scalmani, G.; Barone, V.; Menucci, B.; Petersson, G. A.; et al. *Gaussian 09*, Revision C.01; Gaussian, Inc.: Wallingford, CT, 2010.
(33) Merrick, J. P.; Moran, D.; Radom, L. An Evaluation of Harmonic Vibrational Scale Factors. *J. Phys. Chem. A* **2007**, *111*, 11683.
(34) Piantek, M.; Miguel, J.; Krüger, A.; Navío, C.; Bernien, M.; Ball, D. K.; Hermann, K.; Kuch, W. Temperature, Surface, and Coverage-Induced Conformational Changes of Azobenzene Derivatives on Cu(001). *J. Phys. Chem. C* **2009**, *113*, 20307−20315.
(35) CuNAr abstracts H atoms from the *ortho*-positions rather than those from *meta*- and *para*-positions, suggested by the lack of $Ar'NH_2$ evolution above 500 K when 2,6-difluorophenyl azide (with fluorine substitution at both *ortho*-positions) was utilized as the nitrene precursor (see Figure S3). This preference is probably due to their close proximity to the adjacent nitrogen of the copper/nitrene at the moment of abstraction.
(36) Trogler, W. C. Electronic Structure, and Reactivity of Metallacyclotetraazapentadienes. *Acc. Chem. Res.* **1990**, *23*, 426−431.
(37) Gross, M. E.; Johnson, C. E.; Maroney, M. J.; Trogler, W. C. Photochemistry of Cyclopentadienylcobalt 1,4-Diaryltetraazadienes. Examples of C-H, C-F, and C-C Bond Breaking. *Inorg. Chem.* **1984**, *23*, 2968−2973.
(38) Schrock, A. K.; Schuster, G. B. Photochemistry of Phenyl Azide: Chemical Properties of the Transient Intermediates. *J. Am. Chem. Soc.* **1984**, *106*, 5228−5234.
(39) Leyva, E.; Platz, M. S.; Persy, G.; Wirz, J. Photochemistry of Phenyl Azide: The Role of Singlet and Triplet Phenylnitrene as Transient Intermediates. *J. Am. Chem. Soc.* **1986**, *108*, 3783−3790.
(40) Gritsan, N. P.; Tigelaar, D.; Platz, M. S. A Laser Flash Photolysis Study of Some Simple Para-Substituted Derivatives of Singlet Phenyl Nitrene. *J. Phys. Chem. A* **1999**, *103*, 4465−4469.
(41) McCusker, C. E.; Hablot, D.; Ziessel, R.; Castellano, F. N. Metal Coordination Induced π-Extension and Triplet State Production in Diketopyrrolopyrrole Chromophores. *Inorg. Chem.* **2012**, *51*, 7957−7959.
(42) Zhu, X.-L.; White, J. M. In *Laser Spectroscopy and Photochemistry on Metal Surfaces Part II*; Dai, H.-L., Ho, W., Eds.; World Scientific: Singapore, 1995; pp 1141−1240.
(43) Kahn, A. Fermi Level, Work Function and Vacuum Level. *Mater. Horiz.* **2016**, *3*, 7−10.
(44) Ukraintsev, V.; Long, T. J.; Harrison, I. Photofragmentation Dynamics of Submonolayers of CH_3Br Adsorbed on Pt(111). *J. Chem. Phys.* **1992**, *96*, 3957−3965.
(45) Gartland, P. O.; Berge, S.; Slagsvold, B. J. Photoelectric Work Function of a Copper Single Crystal for the (100), (110), (111), and (112) Faces. *Phys. Rev. Lett.* **1972**, *28*, 738−739.
(46) Witte, G.; Lukas, S.; Bagus, P. S.; Wöll, C. Vacuum Level Alignment at Organic/metal Junctions: Cushion effect and Interface Dipole. *Appl. Phys. Lett.* **2005**, *87*, 263502.
(47) Germer, T. A.; Stephenson, J. C.; Heilweil, E. J.; Cavanagh, R. R. Picosecond Time-Resolved Adsorbate Response to Substrate Heating: Spectroscopy and Dynamics of CO/Cu(100). *J. Chem. Phys.* **1994**, *101*, 1704−1716.

DOI: 10.1021/acs.jpcc.8b12373
J. Phys. Chem. C 2019, 123, 12195−12202